Journal of Operation and Automation in Power Engineering

vol. XX, no. XX, Dec. 2022, Pages: XXXX (Proofed)

http://joape.uma.ac.ir

A Novel Meter Placement Algorithm Based on Monte Carlo Coupled State Estimation and Iterative Nonlinear Mesh Adaptive Direct Search

F. Jabari *, *M. Shabanzadeh, M. Zeraati*

Power Systems Operation and Planning Research Department, Niroo Research Institute (NRI), Shahrak Ghods, Tehran, Iran.

***Abstract*—** *Distribution system state estimation (DSSE) is widely used for real-time monitoring of power grids, where different types of metering devices such as phasor measurement units, smart meters, power quality meters, and etc. are installed. The accuracy of estimated states and the system observability level depends on the type, number and location of meters and since there are many nodes and branches in such large networks, a highly redundant measurement infrastructure is practically unattainable due to the limited investment budget. Hence, this paper proposes a novel meter placement algorithm aiming to minimize the distribution system state estimation error and enhance the system observability level considering the limited number of available meters or investment cost. To this end, on one hand, Monte Carlo simulation (MCS) is applied to a weighted least squares (WLS) based DSSE to find the nodal voltage magnitude and angle as the state variables under the uncertainty of measurements. A MCS and WLS-DSSE hybrid iterative nonlinear optimization mesh adaptive direct search (NOMADS) algorithm is proposed to obtain the best locations of the voltage measuring units considering a trade-off between the DSSE performance and the investment cost. The uncertainties associated with the voltage measurements are modeled using random errors with normal probability distribution function. The efciency and applicability of the proposed method are analyzed by its implementation on a 25-node unbalanced radial distribution system and numerical results demonstrate that this method technically outperforms other heuristic algorithms in the literature which are usually computationally intractable or more demanding in finding the optimal meter places under uncertainties. Compared to other recently developed algorithms, the accuracy of the estimated states as well as the runtime of the proposed algorithm are improved significantly especially under severe measuring errors. Moreover, it is capable to find the minimum number of voltage meters ensuring that the system observability criterion and the expected DSSE accuracy are fulfilled under the uncertain operating conditions.*

***Keywords*—**Distribution system state estimation (DSSE), weighted least squares (WLS), meter placement, nonlinear optimization mesh adaptive direct search (NOMADS).

NOMENCLATURE

Subscripts and superscripts

iter	Iteration of meter placement algorithm
k	Iteration of NOMADS algorithm
v	Iteration of WLS based DSSE method

Symbols

$e_{i,s}^{rand}$	Random error for modelling the uncertainty of the voltage measurement i at Monte Carlo scenario s
$I_{\phi}^{(v)}$	Load current for phase ϕ at iteration of DSSE algorithm
$M\left(k,\Delta_k\right)$	Model of a mesh with size Δ_k at iteration k of NOMADS algorithm
$N_{VM}^{(iter)}$	Voltage meters at iteration iter of meter placement algorithm
$N_{VM}^{\min}$, $N_{VM}^{\max}$	Minimum and maximum number of meters
$P_{\phi}^{Load}, Q_{\phi}^{Load}$	Active and reactive power load for phase ϕ
P_k	A set of trial mesh points at iteration k of NOMADS algorithm
$P_V^{\max}$, $P_{\delta}^{\max}$	Probability of the voltage magnitude/phase angle estimation error violation according to the actual and estimated values of the nodal voltages
v_{ϕ}^{r}, v_{ϕ}^{i}	Real and imaginary parts of nodal voltage for phase ϕ
$V_{\phi}^{(v)}$	Voltage magnitude for phase ϕ at iteration v of DSSE algorithm
V_i^{est}, δ_i^{est}	Actual voltage measurement i at Monte Carlo scenario s
V_i^{LF}	Real and imaginary parts of nodal voltage for phase ϕ
$V_{i,s}^{act}$	Voltage magnitude for phase ϕ at iteration of DSSE algorithm
ε_V, ε_{δ}	Predefined threshold values for relative errors of voltage magnitude and angle between actual and estimated nodal voltages
$c_j(y)$	j-th optimization constraint of NOMDAS algorithm
D_k	Positive spanning set representing $n \times 2n$ directions at iteration k that is modelled as a $\left[-I \quad I\right]_{n\times 2n}$ matrix
I_r, I_i	Real and imaginary parts of branch current
$I_{n\times n}$	Identity matrix
$x^{(v)}$	Estimated voltage magnitude and angle of node i
y_i	Binary variable equal to 1 if there is a voltage meter at node i, otherwise it will be 0
e	Measurements error vector
G	Gain matrix of DSSE algorithm
H	Measurements Jacobian matrix
J(x)	Objective function of DSSE algorithm (i.e., weighted least squares of estimation errors)

Received: 06 May 2023
Revised: 02 Jul. 2023
Accepted: 27 Aug. 2023
*Corresponding author:
E-mail: fjabbari@nri.ac.ir (F. Jabari)
DOI: 10.22098/joape.2023.12842.1976
Research Paper

m	Total number of measurements
W	Voltage of node i obtained from the backward-forward sweep load flow method
Y	Binary decision vector in meter placement process
z	Measurement vector

1. INTRODUCTION

Nowadays, increasing rate of energy demand and uncertainties associated with renewable power generation have greatly induce electric distribution networks to be operated close to their stability margins [1]. Hence, real-time monitoring of power distribution systems is absolutely essential for effective control and protection actions [2, 3]. However, as in realistic distribution feeders, there are a large number of nodes and branches, it is not economical to install the metering devices such as smart meters, micro phasor measurement units (μPMUs), and power quality monitors (PQMs) at all nodes or branches [4, 5]. In this way, distribution system state estimation (DSSE) methods are usually used for processing the limited number of actual measurements under a given network topology to estimate all nodal voltages and branch currents [6]. In other hand, depending on how many measurement points exist in a grid, the DSSE algorithm may or may not converge to a state estimation [7]. A system is called observable when there are adequate measurements for estimating its state variables (i.e., magnitude and phase angle of nodal voltages or branch currents) with minimum errors but distribution networks are mostly unobservable due to the lack of actual measurements [8]. To deal with this problem, many pseudo measurements with high variance (e.g., load forecasts) must be used in the DSSE algorithm as the input data to make the network observable. Mathematically, an observable network is generally a determined system in which the number of measurement points is equal to the number of state variables [9]. In such systems, there is no redundancy in measurement set and thus, one exact solution can be found as the systems state. Nevertheless, since the type, number and location of actual measurements affect the accuracy of DSSE module [10], a meter placement algorithm should be adopted to optimally determine the location of new meters in distribution networks with the aim of achieving a fully-observable system [11].

The meter placement problem has been first introduced in the work of Schweppe and Wildes [12]. In this research, the measurement covariance matrix is used for solving both DSSE and meter placement problems. Some notable works focusing on μPMUs and smart meters placement in power distribution systems are also extended in [13–16]. In [17, 18], a mixed integer linear programming (MILP) problem is solved to allocate the voltage and power measurements in radial feeders. Sum of node voltage estimation errors is minimized considering the maximum number of voltage and flow meters as well as the investment cost limit. In [18], uncertainties associated with the distributed energy resources (DER) and loads are also included in the allocation process. An integer linear programming model is developed in [19] for optimal ţPMU placement in order to maintain network observable following a reconfiguration in distribution network considering the limited current and voltage measurement channels. In [20], a data-based method is described for optimal sensor placement to observe the system states based on the proper orthogonal decomposition approach using a limited number of measurements. A real-time and computationally efficient state estimation algorithm is developed in [21] for distribution networks using PMUs which can detect and identify the anomalies such as bad date and sudden load changes.

In [10], a probability index is introduced to find the most appropriate places for meters installation. This index is calculated based on maximum relative errors between the actual and estimated values of voltage magnitude and phase angle as well as the active and reactive power flows of lines under different Monte Carlo simulation (MCS) scenarios. In the proposed model, uncertainties of loads and also actual measurements data are randomly generated by 100 runs of MCS. At each meter placement scenario, the relative errors of voltage magnitude and phase angle are calculated for all network nodes. A node with maximum relative error between its actual and estimated voltage values is selected as candidate for installation of voltage measuring devices. Similarly, the relative errors of active and reactive power flows of the branches are determined as Monte Carlo iterations progress, according to which a flow meter is then installed at a line with the maximum area of the error ellipse.

In [22], the authors have mentioned that there are four important aspects for distribution operators to prefer some specific places to others for the purpose of installing metering devices: (1) branches with high power capacity, (2) branches with high power losses, (3) measurements in branches with frequently changes of power flow direction, (4) main feeders, which directly feed several connected laterals. With this aim in mind, the operational priority indices, investment costs, relative errors of voltage magnitude and phase, and also network observability are considered as objectives of the meter placement problem. Moreover, in their work, relative errors of node voltage magnitude and phase assumed to be 1% and 5%, respectively. Authors of [23, 24] have supposed that there are two types of metering devices, μPMUs and smart meters, to be installed in distribution networks. In their work, total cost of μPMUs and smart meters as well as relative errors of nodal voltage magnitude and phase angle are simultaneously minimized using a GA based on N-1 degradation robustness approach and a hybrid particle swarm optimization (PSO)-Krill Herd algorithm (KHA). In addition, they have restricted the relative errors of the voltage magnitude and phase using two inequality constraints. More importantly, the stochastic nature of photovoltaic panels and wind farms generation is also included in a robust optimization scheme. In [25], sum of diagonal elements of covariance error matrix is considered as an objective function to be minimized. The main focus of this research is that since a fully-observable n-bus grid is fulfilled by allocating (n-1) number of measurements, the observability of distribution feeder can only be satisfied if the rank of Jacobian matrix is greater than (n-1). To develop previous works, Wang et al. [26] solved a robust meter placement problem considering uncertainties associated with output powers of distributed generations (DGs) and various network reconfiguration scenarios using Markov chain and Gaussian mixture model (GMM). Additionally, MCS is run to model uncertainties originated by the inherent inaccuracy of measurements. In this work, the total cost of the metering infrastructure is limited to an investment budget with the aim of minimizing the average value of maximum relative errors of the nodal voltages in MCS. In the same vein, in [27], an interior point method is combined with DSSE algorithm to minimize the total investment cost of power flow and voltage magnitude meters, as well as sum of the average value of nodal voltage magnitude and phase relative errors, obtained over MCS process, for all network nodes.

Raposo et al. [28] have considered the correlated measurements, multiple load levels and also the accuracy of estimation results to find an optimal measurement system design. Toward this aim, they have also employed binary particle swarm optimization (BPSO) algorithm. Further, they have introduced a probabilistic risk index, which limits the maximum voltage magnitude and phase errors to 1% and 5%, respectively. In their proposed model, the maximum number of different types of meters is also considered as a constraint to lead the algorithm toward an adequate solution vector with the minimum investment cost. In [29], the ellipsoid area of the estimation error is minimized to improve the accuracy of DSSE using a mixed-integer semi-definite programming method. In [11], a limited number of voltage magnitude meters and μPMUs is assumed to be available in the distribution network, according to which the accuracy of DSSE algorithm is investigated by tracing the inverse of Fisher information matrix. This work has shown that the Greedy algorithm is able to find a near-optimal solution with minimum total estimation variance for meter placement problem.

Othman et al. [30] have presented a rule for installation of smart meters in distribution systems. A reference meter is placed at the HV/MV substation for concentrating some key information of the feeders and their laterals (e.g., branch topologies, impedances, line currents and power flows, voltage profile, load levels, and power losses) from all individual smart meters. In this proposed approach, the nodes located at the beginning and end of the farthest laterals of each feeder are suggested as candidate points for installing smart meters.

Another relevant issue is discussed in [31], which a seeker optimization technique is employed for optimal allocation of power quality (PQ) meters. In this model, the weighted sum of the maximum relative errors of harmonic voltage values is minimized considering a limited number of PQ measuring units. In [32], an optimal ţPMU placement algorithm is proposed to be applicable in radial distribution networks, taking into account the uncertainties of the configuration and topology of their feeders. From a technical viewpoint, data security and system observability is evaluated in [33] using a bi-level optimization model. At the upper level, optimum locations of μPMUs are found considering the observability of nodes and the investment cost of measurement system. Owing to some security issues, it is assumed that all μPMUs should be covered at least by one firewall to ensure their secure data exchange. Hence, a security index is defined for all nodes and must be maximized in the lower level. In [34], a weighted least square (WLS)-based DSSE algorithm is developed introducing virtual meters concept. It is assumed that a virtual meter is installed at each node except the slack bus (i.e., the HV/MV substation), which results in higher accuracy and lower calculation time in DSSE convergence. Mazlumi et al. [35] have proved that data security and system observability can be improved, especially in case of line or μPMU outages, if some single-channel μPMUs are placed at the beginning points of candidate branches. In [36], it is suggested that PMUs data are used for solving the DSSE algorithm in balanced multi-area distribution systems. For this purpose, the main system must be separated into several sub-systems based on μPMUs locations. Then, DSSE algorithm is run for each area to estimate all its local state variables. These estimated values along with actual measurements can be used to solve the integrated DSSE for the primary grid.

The problem addressed in this paper is of high practical significance for any power distribution company. As reviewed in recently published works, there are some heuristic approaches for optimal placement of different types of metering devices such as PQ monitors, μPMUs, smart meters, and so on. But, uncertainties associated with actual measurements have not be well modeled yet; especially, the conventional meters for measuring the voltage magnitude of nodes as well as the active and reactive power flows of lines. Moreover, most of these approaches do not consider the trade-off between accuracy of DSSE algorithm and computational complexity of meter placement process. Hence, this paper presents a simple, straightforward and efficient meter placement approach for application in radial distribution feeders considering the actual measurements uncertainties/errors and enhancing modeling accuracy of the DSSE-based optimization technique. The novelties of the present research are summarized as follows:

- A nonlinear optimization mesh adaptive direct search (NOMADS) algorithm is developed for optimal allocation of voltage magnitude and phase angle measuring units in medium-voltage radial distribution feeders. Compared to other recently published works, this optimization procedure minimizes sum of weighted squares of DSSE errors considering a limited number of voltage measurements under uncertain operating condition. It is supposed that there is a smart meter in bus 1 (slack node). In the first iteration of the NOMADS algorithm, the locations of the available meters as well as the maximum number of voltage meters, which could be installed at network nodes, are determined by the distribution system operator (DSO).
- In each meter placement scenario generated by NOMADS, a number of Monte Carlo simulations (MCS) are run to calculate the probability of the voltage magnitude/phase angle estimation error violation based on actual and estimated values of nodal voltages. In other words, the actual measurements matrix is updated at each iteration of NOMADS algorithm according to the randomly generated binary decision variables, which indicate the installation states of the voltage meters at network nodes. Then, a number of MCS is run for each iteration of NOMADS algorithm to generate a random error with normal distribution function for each actual measurement.
- At each MCS, a weighted least squares based DSSE algorithm is run to find optimal values of system states (magnitude and angle of nodal voltages) and their relative errors according to actual voltages. The maximum relative errors of the node voltage magnitude/phase are calculated based on the actual voltage measurements. If these values are less than 1% for voltage magnitude and 5% for voltage phase, a feasible solution is found for allocating meters; otherwise another meter placement scenario will be generated by NOMADS algorithm. If a feasible solution is obtained for meter locations, the maximum number of meters required for making the distribution system full observable will be updated as equal to minimum value of (a) and (b), where: (a) the number of primary meters (determined by DSO) and (b) the sum of binary decision variables obtained in this solution (indicating the installation status of voltage meters). Otherwise, if an infeasible solution is found and the optimization constraints are not fulfilled, the minimum required voltage meters will be calculated as the maximum value of (c) and (d), where: (c) the number of primary meters (determined by DSO) and (d) minimum required meters (at iteration 1, this value is considered as the number of available meters before implementation of the placement strategy; at other iterations, it is calculated as minimum of (c) and (d)).
- After updating the minimum and maximum numbers of the voltage measurements, the number of meters will be updated as:
  round((minimum number of meters + maximum number of meters)/2)
  Then, meter placement solution is updated to be used as the initial solution vector in NOMADS optimization algorithm. This process is repeated until the minimum number of the voltage measuring units is found in a way that the maximum relative errors of the voltage magnitude and phase among all nodes for at least 80% of MCS would be less than 1% and 5%, respectively.
- Simulations are conducted on a 25-node radial distribution system to find the best measuring scheme for the installation of the voltage magnitude and phase angle metering devices. Numerical analyses are finally presented to reveal the higher accuracy and lower computational burden of the proposed approach in comparison with other recently introduced algorithms.

Other parts of this paper is organized as follows. In Section 2, the proposed meter placement algorithm is presented to illustrate performance gains of using WLS-based DSSE and NOMADS optimization methods. A case study and its numerical results are evaluated and discussed in Section 3. Finally, some concluding remarks and future trends are stated in Section 4.

2. PROPOSED METER PLACEMENT STRATEGY

In the branch-current based DSSE approach, the measurement vector z is defined using the state vector x and the measurement error vector e, as formulated by Eq. (1).

$$z = h(x) + e \tag{1}$$

where, $h(x)$ is the function of the measurement matrix which relates the measurements to the state variables. According to Eq. (2), the real and imaginary parts of the branch current are considered as the state variables.

$$x = [I_r,\ I_i] \tag{2}$$

The performance of the DSSE algorithm is evaluated by the weighted least squares (WLS), as given by Eq. (3).

$$J(x) = \sum\nolimits_{i=1}^{m} w_i \left(z_i - h_i\left(x\right)\right)^2 = [z - h(x)]^T W\,[z - h(x)] \tag{3}$$

The weighting matrix and the total number of actual and pseudo measurements are denoted by W and m, respectively. As calculated in Eqs. (4)-(6), the decision variables of the DSSE algorithm at each iteration v can be found when the 1st-order derivation of the objective function $J(x)$ is zero.

$$\begin{aligned} &g(x) = \partial J(x)/\partial x = -H^T(x)W[z - h(x)] = 0; \\ &H(x) = \partial h(x) = \partial h(x)/\partial x \end{aligned} \tag{4}$$

$$x^{(v+1)} = x^{(v)} - \left[G\left(x^{(v)}\right)\right]^{-1} G\left(x^{(v)}\right) \tag{5}$$

$$G\left(x^{(v)}\right) = \partial g(x)/\partial x = H^T(x).W.H(x) \tag{6}$$

Where, Jacobian and Gain matrices are indicated by H and G, respectively. It is supposed that the values of active and reactive loads are pseudo measurements. These values are stated in the form of a three-phase current using Eq. (7) to be simply used in the branch-current based DSSE algorithm.

$$I_\phi^{(v)} = \left[\frac{P_\phi^{Load} - jQ_\phi^{Load}}{V_\phi^{(v)}}\right]^* \ ;\ \ \forall \phi \in \{a, b, c\} \tag{7}$$

where, $V_\phi^{(v)}$ is the three-phase nodal voltage magnitude at iteration of the state estimation process. To involve the role of each measurement (both actual and pseudo ones) in the three-phase DSSE solution, a weighting matrix needs to be also defined; as shown in Eqs. (8) and (9).

$$\begin{bmatrix} \Delta I_a^r \\ \Delta I_b^r \\ \Delta I_c^r \\ \Delta I_a^i \\ \Delta I_b^i \\ \Delta I_c^i \end{bmatrix}^{(v)} = \left[G\left(I^{(v)}\right)\right]^{-1}.H^T\left(I^{(v)}\right) .W. \begin{bmatrix} \Delta I_a^r \\ \Delta I_b^r \\ \Delta I_c^r \\ \Delta I_a^i \\ \Delta I_b^i \\ \Delta I_c^i \\ \Delta V_a^r \\ \Delta V_b^r \\ \Delta V_c^r \\ \Delta V_a^i \\ \Delta V_b^i \\ \Delta V_c^i \end{bmatrix}^{(v)} \tag{8}$$

$$\mathrm{W}= \begin{bmatrix} W_{Ia}^r & 0 & 0 & 0 & 0 & 0 & 0 & 0 & 0 & 0 & 0 & 0 \\ 0 & W_{Ia}^r & 0 & 0 & 0 & 0 & 0 & 0 & 0 & 0 & 0 & 0 \\ 0 & 0 & W_{Ic}^r & 0 & 0 & 0 & 0 & 0 & 0 & 0 & 0 & 0 \\ 0 & 0 & 0 & W_{Ia}^i & 0 & 0 & 0 & 0 & 0 & 0 & 0 & 0 \\ 0 & 0 & 0 & 0 & W_{Ib}^i & 0 & 0 & 0 & 0 & 0 & 0 & 0 \\ 0 & 0 & 0 & 0 & 0 & W_{Ic}^i & 0 & 0 & 0 & 0 & 0 & 0 \\ 0 & 0 & 0 & 0 & 0 & 0 & W_{va}^r & 0 & 0 & 0 & 0 & 0 \\ 0 & 0 & 0 & 0 & 0 & 0 & 0 & W_{vb}^r & 0 & 0 & 0 & 0 \\ 0 & 0 & 0 & 0 & 0 & 0 & 0 & 0 & W_{vc}^r & 0 & 0 & 0 \\ 0 & 0 & 0 & 0 & 0 & 0 & 0 & 0 & 0 & W_{va}^i & 0 & 0 \\ 0 & 0 & 0 & 0 & 0 & 0 & 0 & 0 & 0 & 0 & W_{vb}^i & 0 \\ 0 & 0 & 0 & 0 & 0 & 0 & 0 & 0 & 0 & 0 & 0 & W_{vc}^i \end{bmatrix} \tag{9}$$

Accordingly, the Jacobian matrix of the state estimation algorithm can be calculated as Eq. (10). In the mesh adaptive direct search optimization algorithm, the objective function $f(y)$ with the decision variables y is minimized as Eq. (11) [37].

$$H = \begin{bmatrix} \frac{\partial I_a^r}{\partial I_a^r} & \frac{\partial I_a^r}{\partial I_b^r} & \frac{\partial I_a^r}{\partial I_c^r} & \frac{\partial I_a^r}{\partial I_a^i} & \frac{\partial I_a^r}{\partial I_b^i} & \frac{\partial I_a^r}{\partial I_c^i} \\ \frac{\partial I_b^r}{\partial I_a^r} & \frac{\partial I_b^r}{\partial I_b^r} & \frac{\partial I_b^r}{\partial I_c^r} & \frac{\partial I_b^r}{\partial I_a^i} & \frac{\partial I_b^r}{\partial I_b^i} & \frac{\partial I_b^r}{\partial I_c^i} \\ \frac{\partial I_c^r}{\partial I_a^r} & \frac{\partial I_c^r}{\partial I_b^r} & \frac{\partial I_c^r}{\partial I_c^r} & \frac{\partial I_c^r}{\partial I_a^i} & \frac{\partial I_c^r}{\partial I_b^i} & \frac{\partial I_c^r}{\partial I_c^i} \\ \frac{\partial I_a^i}{\partial I_a^r} & \frac{\partial I_a^i}{\partial I_b^r} & \frac{\partial I_a^i}{\partial I_c^r} & \frac{\partial I_a^i}{\partial I_a^i} & \frac{\partial I_a^i}{\partial I_b^i} & \frac{\partial I_a^i}{\partial I_c^i} \\ \frac{\partial I_b^i}{\partial I_a^r} & \frac{\partial I_b^i}{\partial I_b^r} & \frac{\partial I_b^i}{\partial I_c^r} & \frac{\partial I_b^i}{\partial I_a^i} & \frac{\partial I_b^i}{\partial I_b^i} & \frac{\partial I_b^i}{\partial I_c^i} \\ \frac{\partial I_c^i}{\partial I_a^r} & \frac{\partial I_c^i}{\partial I_b^r} & \frac{\partial I_c^i}{\partial I_c^r} & \frac{\partial I_c^i}{\partial I_a^i} & \frac{\partial I_c^i}{\partial I_b^i} & \frac{\partial I_c^i}{\partial I_c^i} \\ \frac{\partial I_a^r}{\partial I_a^r} & \frac{\partial I_a^r}{\partial I_b^r} & \frac{\partial I_a^r}{\partial I_c^r} & \frac{\partial I_a^r}{\partial I_a^i} & \frac{\partial I_a^r}{\partial I_b^i} & \frac{\partial I_a^r}{\partial I_c^i} \\ \frac{\partial I_b^r}{\partial I_a^r} & \frac{\partial I_b^r}{\partial I_b^r} & \frac{\partial I_b^r}{\partial I_c^r} & \frac{\partial I_b^r}{\partial I_a^i} & \frac{\partial I_b^r}{\partial I_b^i} & \frac{\partial I_b^r}{\partial I_c^i} \\ \frac{\partial I_c^r}{\partial I_a^r} & \frac{\partial I_c^r}{\partial I_b^r} & \frac{\partial I_c^r}{\partial I_c^r} & \frac{\partial I_c^r}{\partial I_a^i} & \frac{\partial I_c^r}{\partial I_b^i} & \frac{\partial I_c^r}{\partial I_c^i} \\ \frac{\partial I_a^i}{\partial I_a^r} & \frac{\partial I_a^i}{\partial I_b^r} & \frac{\partial I_a^i}{\partial I_c^r} & \frac{\partial I_a^i}{\partial I_a^i} & \frac{\partial I_a^i}{\partial I_b^i} & \frac{\partial I_a^i}{\partial I_c^i} \\ \frac{\partial I_b^i}{\partial I_a^r} & \frac{\partial I_b^i}{\partial I_b^r} & \frac{\partial I_b^i}{\partial I_c^r} & \frac{\partial I_b^i}{\partial I_a^i} & \frac{\partial I_b^i}{\partial I_b^i} & \frac{\partial I_b^i}{\partial I_c^i} \\ \frac{\partial I_c^i}{\partial I_a^r} & \frac{\partial I_c^i}{\partial I_b^r} & \frac{\partial I_c^i}{\partial I_c^r} & \frac{\partial I_c^i}{\partial I_a^i} & \frac{\partial I_c^i}{\partial I_b^i} & \frac{\partial I_c^i}{\partial I_c^i} \end{bmatrix} \tag{10}$$

$$\min_{y \in \Omega \subseteq \mathbb{R}^n} f\left(y\right) \tag{11}$$

In which, $f : \mathbb{R}^n \rightarrow \mathbb{R} \cup \{\infty\}$, $\Omega = \{y \in Y : c_j\left(y\right) \leq 0;\ j = 1, 2, ..., l\}$ and $Y \subseteq \mathbb{R}^n$ represents the closed or bounded constraints of the decision variables y. Moreover, $c_j(y) : \mathbb{R}^n \rightarrow \mathbb{R}$ for $j = 1, 2, ..., l$ models other optimization limitations or open constraints. To solve such a big decision-making problem aected by uncertain input data, the method of NOMADS can constitute a powerful solution alternative. It is an iterative algorithm using a mesh with discrete structure, which is modeled at each iteration k as Eq. (12) [37].

$$M\left(k,\ \Delta_k\right) = \cup_{y \in \psi_k} \left\{Y + \Delta_k D_k\right\} \subseteq \mathbb{R}^n \tag{12}$$

where, the parameter $\Delta_k \in \mathbb{R}^+$ refers the mesh size, D_k is a positive spanning set representing $n \times 2n$ directions in $\mathbb{R}^n$ that is generally modeled as a $\begin{bmatrix} -I & I \end{bmatrix}_{n \times 2n}$ matrix. It should be noted that I is an $n \times n$ identity matrix. In addition, ψ_k represents the set of points for assessing both objective function and constraints at iteration k. It is assumed that all trial mesh points belongs to a compact set, for instance, set ω, and each mesh is constructed using integer combinations of $\Delta_k D$. Hence, there is a finite number of points in $\omega \cap M\left(k, \Delta_k\right)$. As illustrated in Fig. 1, each iteration of mesh adaptive direct search consists of two steps, namely, poll and search. In the search step, the objective function is evaluated on a finite number of points of mesh $M\left(k, \Delta_k\right)$ using the variable neighborhood search (VNS) [37]. The set of trial mesh points included in the poll step, called a frame, is also constructed as P_k using Eq. (13). The objective function is then evaluated on n_D points of P_k. The parameter D_k

models the set of directions involved in construction of the frame P_k.

$$P_k = \{Y + \Delta_k d : d \in D_k\} \tag{13}$$

If a trial mesh point with lower objective function than that explored previously is found, it is called an improved mesh point resulting a successful iteration. Hence, the mesh size parameter and the solution are updated using Eqs. (14) and (15), respectively.

$$\Delta_{k+1} = \tau^{w_k} \times \Delta_k \tag{14}$$

$$Y_{k+1} = Y_k \times \Delta_k D_k \tag{15}$$

Note that $\tau \rangle 1$ is a fixed reasonable number. In addition, w_k is a positive finite integer if k^{th} iteration is marked success; otherwise, it will be negative. The mesh size will be decreased after failures and increased while a successful iteration is found. As mentioned before, D_{k+1} is an identity matrix at iteration $k+1$, which is shown as $\begin{bmatrix} -I & I \end{bmatrix}_{n \times 2n}$.$A$ binary decision vector is defined as Eq. (16), where, y_i denotes the installation status of the voltage meter at node i and Ω_B is the set of network nodes. If a voltage measuring unit is placed at node i, y_i will be equal to 1; else it is 0.

$$Y = [y_1,\, y_2,\, ...,\, y_i,\, ...\, y_N]\ ;\ i \in \Omega_B \tag{16}$$

To find the binary decision vector Y, the lower and upper bound of the integer decision variables y_i should be set to 0 and 1, respectively. Before adopting the optimal meter placement strategy, if there is a voltage meter at node j, the lower bound of the decision variable y_j will be equal to 1. Taking into account this trick, the initial decision vector y must be primarily updated. Afterwards, considering the investment budget on the one hand, and the voltage meter cost on the other hand, the maximum number of measuring devices, which can be added to the metering infrastructure, is determined by DSO as $N_{VM}^{\max}$. In the first scenario of the NOMADS optimization algorithm, the number of voltage meters is updated using $N_{VM}^{iter=1} = N_{VM}^{\max}$. Meanwhile, the minimum $\left(N_{VM}^{\min}\right)$ and maximum $\left(N_{VM}^{\max}\right)$ numbers of meters are determined based on available measurements in the distribution network. For example, if there are two voltage meters at nodes 1 and 5, initial values of these variables must be set to $N_{VM}^{\min} = N_{VM}^{\max} = 2$. Also, a stopping criterion is defined for the NOMADS optimization method as $stop_{opt}$, which initially equals to 0 and changes into 1 when the algorithm converges to the best solution. While $stop_{opt} = 0$, the MCS-based DSSE algorithm is run taking into account the binary state vector y. Indeed, this algorithm is run by applying the binary state variables x_i to the node voltage measurement matrix as Eq. (17).

$$V_{i,\,s}^{act} = \left(1 + e_{i,\,s}^{rand}\right) \times V_i^{LF};\ \ \forall i \in \Omega_B,\ \ x_i = 1 \tag{17}$$

If there is a voltage meter at node $i(i.e., y_i = 1)$, the random error $e_{i,s}^{rand}$ is used to model the uncertainty of the voltage measurement i at Monte Carlo scenario s, which is either a positive or negative coefficient taking into account the accuracy of the voltage meters. The nodal voltages obtained from the load flow algorithm $\left(V_i^{LF}\right)$ are also used to generate uncertain values as the actual voltage measurements $\left(V_{i,s}^{act}\right)$.

The observability of distribution system is investigated at each iteration of NOMADS optimization algorithm. As can be modeled by Eq. (18), if the gain matrix G is not singular, the WLS algorithm can estimate the network state variables and thereby, the system could be full-observable. Otherwise, another solution should be generated by the NOMADS algorithm.

$$\det\{G(x)\} \neq 0 \tag{18}$$

The probability of the voltage magnitude/phase angle estimation error violation is calculated based on actual and estimated values of nodal voltages, as given by Eq. (19). In this study, it is assumed that $\varepsilon_V = 1\%$, $\varepsilon_\delta = 5\%$ [28], and $P_V = P_\delta = 0.2$.

$$\begin{aligned} P_V^{\max} &= \max_{i \in \Omega_B} \left\{ P\left(\left| \frac{V_i^{est} - V_i^{act}}{V_i^{act}} \right| \geq \varepsilon_V \right) \right\} \leq p_V, \\ P_\delta^{\max} &= \max_{i \in \Omega_B} \left\{ P\left(\left| \frac{\delta_i^{est} - \delta_i^{act}}{\delta_i^{act}} \right| \geq \varepsilon_\delta \right) \right\} \leq p_\delta \end{aligned} \tag{19}$$

After running a large number of MCS (for example, 1000 scenarios), if both risk indices $P_V^{\max}$ and $P_\delta^{\max}$ are less than a predefined probability (here, 20%), this binary solution vector is saved as a feasible meter placement scenario. Hence, the maximum number of meters is updated as Eq. (20). Otherwise, if the constraint Eq. (19) is not fulfilled, a feasible solution will not be found and the minimum number of meters should be updated as Eq. (21).

$$N_{VM}^{\max} = \min\left(N_{VM}^{(iter)},\, \sum\nolimits_{i \in \Omega_B} y_i\right) \tag{20}$$

$$N_{VM}^{\min} = \max\left(N_{VM}^{(iter)},\, N_{VM}^{\min}\right) \tag{21}$$

The number of meters is then updated using Eqs. (20) and (21), as modeled in Eq. (22).

$$N_{VM}^{(iter+1)} = round\left\{0.5 \times \left(N_{VM}^{\min},\, N_{VM}^{\max}\right)\right\} \tag{22}$$

If $N_{VM}^{(iter+1)} = N_{VM}^{(iter)}$, the optimization algorithm is converged to the best solution finding the minimum number of the voltage measuring units, as stated in Eq. (22).

$$Objective\ function = \sum\nolimits_{i \in \Omega_B} y_i \tag{23}$$

3. ILLUSTRATIVE EXAMPLE, NUMERICAL RESULTS AND DISCUSSIONS

In this section, the proposed meter placement algorithm, illustrated through the owchart depicted in Fig. 1, is applied to the IEEE unbalanced 25-node radial distribution test system. The nominal voltage and base power of the benchmark feeder are $20kV$ and $1MVA$, respectively. The single-line diagram of this medium-voltage feeder is illustrated in Fig. 2 [38]. The active and reactive loads are reported in Table 1. Five impedance matrices shown in Fig. 2, are considered as below:

$$Z_1 = \begin{bmatrix} 0.0393 + 0.0730i & 0.0018 + 0.0161i & 0.0018 + 0.0161i \\ 0.0018 + 0.0161i & 0.04 + 0.0716i & 0.002 + 0.03i \\ 0.0018 + 0.0161i & 0.002 + 0.03i & 0.04 + 0.0723i \end{bmatrix}$$

$$Z_2 = \begin{bmatrix} 0.1042 + 0.0930i & 0.0018 + 0.0181i & 0.0016 + 0.0135i \\ 0.0018 + 0.0181i & 0.1050 + 0.0922i & 0.002 + 0.0242i \\ 0.0016 + 0.0135i & 0.002 + 0.0242i & 0.1048 + 0.0922i \end{bmatrix}$$

$$Z_3 = \begin{bmatrix} 0.2055 + 0.1513i & 0.0016 + 0.0135i & 0.0016 + 0.0135i \\ 0.0016 + 0.0135i & 0.2055 + 0.1513i & 0.0016 + 0.0135i \\ 0.0016 + 0.0135i & 0.002 + 0.0242i & 0.2055 + 0.1513i \end{bmatrix}$$

$$Z_4 = \begin{bmatrix} 0.1042 + 0.093i & 0.0016 + 0.0135i & 0.0016 + 0.0135i \\ 0.0016 + 0.0135i & 0.1048 + 0.0922i & 0.0016 + 0.0135i \\ 0.0016 + 0.0135i & 0.002 + 0.0242i & 0.1048 + 0.0922i \end{bmatrix}$$

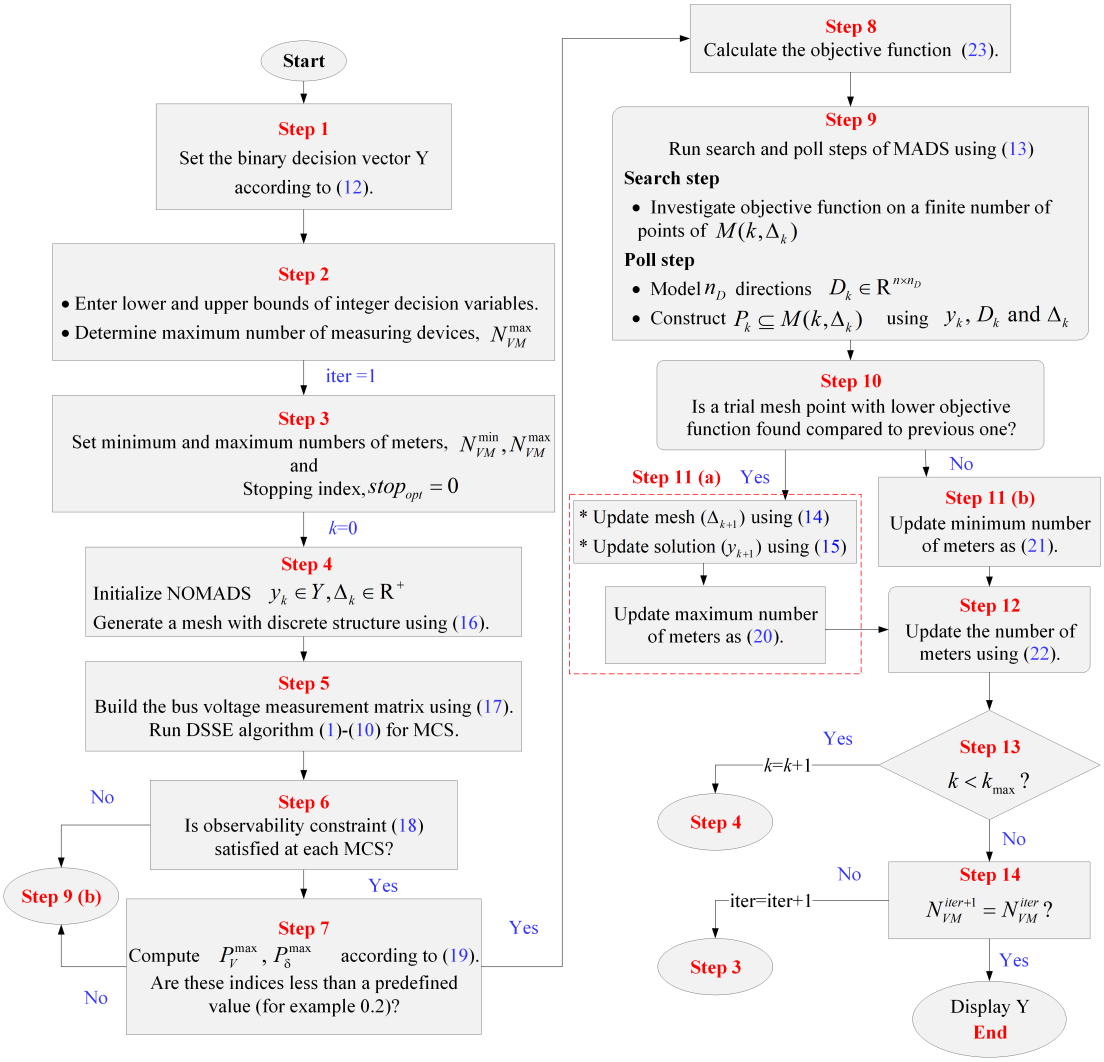

Fig. 1. The flowchart of the proposed meter placement algorithm.

$$Z_5 = \begin{bmatrix} 0.1042+0.093i & 0.0016+0.0135i & 0.0016+0.0135i \\ 0.0016+0.0135i & 0.1042+0.093i & 0.0016+0.0135i \\ 0.0016+0.0135i & 0.002+0.0242i & 0.1048+0.0922i \end{bmatrix}$$

The branch data of this system is also presented in Table 2. In this study, the numerical results obtained from the forward-backward sweep (FBS) load flow of radial distribution systems are analyzed to assess the accuracy of the estimated states (i.e., nodal voltages). With this aim in mind, the load flow results obtained for the node voltage magnitude and phase angle are also used to generate the actual voltage measurements with a random measurement error at each MCS. In other words, if the NOMADS algorithm generates a meter placement solution indicating that there is a voltage meter at node k, the actual voltage measurement of the node k at each MCS is generated by applying a random variable error on its voltage vector obtained from the FBS load flow. To this end, the load flow results of the test distribution feeder are reported in Tables 3 and 4 to be used for making the actual voltage measurements at each MCS and investigating the robustness and effectiveness of the optimum meter placement solution. It should be noted that all simulations are coded in MATLAB R2020b and run on a windows-based laptop with a processor clocking at 2.10 GHz and 4 GB of RAM. Maximum standard errors of actual voltage measurements and pseudo measurements are considered as 1% and 50%, respectively [17]. It is also assumed that there are two exiting voltage meters at nodes 1 and 5. Moreover, there is a current meter at branch 1-2. Note also that the default parameters used in NOMADS solver [39] are considered for simulations.

At each iteration of NOMADS algorithm, the DSSE algorithm Eqs. (1)-(10) is run for 1000 MCS updating the nodal voltage measurement matrix according to the generated meter placement solution. The observability of distribution system is then evaluated at each scenario using Eq. (18). If the violation probability of the voltage magnitude/angle estimation error in 1000 MCS is less than 0.2 and the constraint Eq. (19) is satisfied for all full-observable MCS, this solution will be marked as feasible for the meter placement problem, which may be economic or not.

-1cm)

The proposed algorithm is applied to the 25-node test system in a case study with maximum three voltage measuring units. In other words, one additional meter should optimally be placed in the test system considering the observability criterion in Eq. (18) and the limitations of the nodal voltages relative errors of Eq. (19) in 1000 MCS of each NOMADS iteration. Hence, the binary decision variables related to the nodes 1 and 5 are considered to be 1. In this case, the optimization algorithm is not converged to a feasible solution. In fact, for more than 20% MCS of each NOMADS scenario, the maximum relative errors of the node voltage magnitude and angle are not less than 0.01 and 0.05, respectively. Hence, the minimum number of the voltage measurements is updated to be four. Simulations are repeated

Table 1. The active and reactive loads of the distribution test feeder.

Node number	Active power (p.u.)	Reactive power (p.u.)	Node number	Active power (p.u.)	Reactive power (p.u.)
1	0	0	14	0.0035	0.0017
2	0	0	15	0.0355	0.017
3	0	0	16	0	0
4	0	0	17	0	0
5	0.0126	0.0061	18	0.01	0.0049
6	0	0	19	0.004	0.002
7	0	0	20	0.0054	0.0026
8	0.0083	0.004	21	0.0038	0.0018
9	0.0065	0.0032	22	0.0069	0.0033
10	0.0042	0.002	23	0.0063	0.0031
11	0.0044	0.002	24	0.0045	0.0022
12	0.0067	0.0032	25	0.0087	0.0042
13	0.0028	0.0014			

Table 2. The line length of the 25-node radial distribution feeder.

Branch no.	From node	To node	Length (m)	Branch no.	From node	To node	Length (m)
1	1	2	190	13	18	21	76
2	27	3	95	14	4	23	76
3	2	6	95	15	9	10	95
4	3	4	190	16	14	17	57
5	6	7	95	17	14	15	57
6	6	8	190	18	19	20	76
7	3	18	95	19	21	22	76
8	4	5	95	20	23	24	76
9	7	9	95	21	10	11	57
10	7	16	95	22	24	25	76
11	7	14	95	23	11	13	38
12	18	19	95	24	11	12	38

Table 3. Nodal voltages obtained from FBS load flow for 25-node test feeder.

Node number	Voltage of phase a $(\times 10^4 V)$	Voltage of phase b $(\times 10^4 V)$	Voltage of phase c $(\times 10^4 V)$
1	1.1547 + 0.0000i	-0.5774- 1.0000i	-0.5774 + 1.0000i
2	1.1403 - 0.0084i	-0.5738 - 0.9834i	-0.5650 + 0.9945i
3	1.1372 - 0.0102i	-0.5730 - 0.9798i	-0.5624 + 0.9933i
4	1.1342 - 0.0119i	-0.5723 - 0.9763i	-0.5598 + 0.9921i
5	1.1329 - 0.0121i	-0.5718 - 0.9751i	-0.5590 + 0.9912i
6	1.1314 - 0.0098i	-0.5703 - 0.9752i	-0.5596 + 0.9884i
7	1.1238 - 0.0111i	-0.5674 - 0.9682i	-0.5550 + 0.9832i
8	1.1287 - 0.0103i	-0.5693 - 0.9727i	-0.5580 + 0.9865i
9	1.1211 - 0.0116i	-0.5663 - 0.9657i	-0.5534 + 0.9813i
10	1.1191 - 0.0119i	-0.5655 - 0.9638i	-0.5521 + 0.9800i
11	1.1181 - 0.0121i	-0.5652 - 0.9630i	-0.5515 + 0.9793i
12	1.1176 - 0.0121i	-0.5650 - 0.9625i	-0.5512 + 0.9789i
13	1.1178 - 0.0121i	-0.5651 - 0.9626i	-0.5513 + 0.9790i
14	1.1188 - 0.0119i	-0.5654 - 0.9636i	-0.5520 + 0.9798i
15	1.1161 - 0.0124i	-0.5644 - 0.9611i	-0.5504 + 0.9780i
16	1.1238 - 0.0111i	-0.5674 - 0.9682i	-0.5550 + 0.9832i
17	1.1188 - 0.0119i	-0.5654 - 0.9636i	-0.5520 + 0.9798i
18	1.1337 - 0.0108i	-0.5717 - 0.9765i	-0.5602 + 0.9909i
19	1.1326 - 0.0110i	-0.5713 - 0.9755i	-0.5595 + 0.9900i
20	1.1316 - 0.0111i	-0.5709 - 0.9746i	-0.5589 + 0.9892i
21	1.1320 - 0.0110i	-0.5710 - 0.9750i	-0.5592 + 0.9895i
22	1.1310 - 0.0111i	-0.5707 - 0.9740i	-0.5586 + 0.9887i
23	1.1326 - 0.0122i	-0.5717 - 0.9748i	-0.5588 + 0.9910i
24	1.1315 - 0.0124i	-0.5713 - 0.9738i	-0.5581 + 0.9902i
25	1.1302 - 0.0126i	-0.5708 - 0.9726i	-0.5573 + 0.9891i

Table 4. Branch currents for 25-node distribution feeder.

Branch no.	Current of phase a (A)	Current of phase b (A)	Current of phase c (A)
1	11.4835 - 5.7018i	-10.6720 - 7.1453i	-0.8039 +12.7357i
2	4.9827 - 2.4716i	-4.6300 - 3.1030i	-0.3524 + 5.5274i
3	6.5008 - 3.2302i	-6.0421 - 4.0424i	-0.4515 + 7.2083i
4	2.4121 - 1.1990i	-2.2435 - 1.5017i	-0.1686 + 2.6764i
5	5.5324 - 2.7509i	-5.1433 - 3.4395i	-0.3824 + 6.1344i
6	0.9684 - 0.4793i	-0.8987 - 0.6028i	-0.0691 + 1.0739i
7	2.5706 - 1.2726i	-2.3864 - 1.6013i	-0.1838 + 2.8510i
8	0.9641 - 0.4791i	-0.8966 - 0.6003i	-0.0675 + 1.0697i
9	1.9484 - 0.9660i	-1.8090 - 1.2126i	-0.1372 + 2.1595i
10	0.0000 + 0.0000i	0.0000 + 0.0000i	0.0000 + 0.0000i
11	3.5840 - 1.7850i	-3.3343 - 2.2269i	-0.2451 + 3.9750i
12	0.8031 - 0.3974i	-0.7454 - 0.5003i	-0.0576 + 0.8906i
13	0.8035 - 0.3976i	-0.7458 - 0.5006i	-0.0576 + 0.8911i
14	1.4480 - 0.7199i	-1.3470 - 0.9014i	-0.1010 + 1.6067i
15	1.4612 - 0.7241i	-1.3564 - 0.9096i	-0.1032 + 1.6192i
16	0.0000 + 0.0000i	0.0000 + 0.0000i	0.0000 + 0.0000i
17	3.2599 - 1.6247i	-3.0337 - 2.0250i	-0.2220 + 3.6160i
18	0.4828 - 0.2394i	-0.4485 - 0.3006i	-0.0342 + 0.5356i
19	0.4831 - 0.2395i	-0.4488 - 0.3007i	-0.0342 + 0.5359i
20	0.9658 - 0.4803i	-0.8985 - 0.6012i	-0.0673 + 1.0717i
21	1.1372 - 0.5638i	-1.0559 - 0.7077i	-0.0800 + 1.2603i
22	0.6454 - 0.3217i	-0.6011 - 0.4014i	-0.0443 + 0.7166i
23	0.3243 - 0.1605i	-0.3009 - 0.2020i	-0.0231 + 0.3593i
24	0.4886 - 0.2429i	-0.4542 - 0.3038i	-0.0339 + 0.5418i

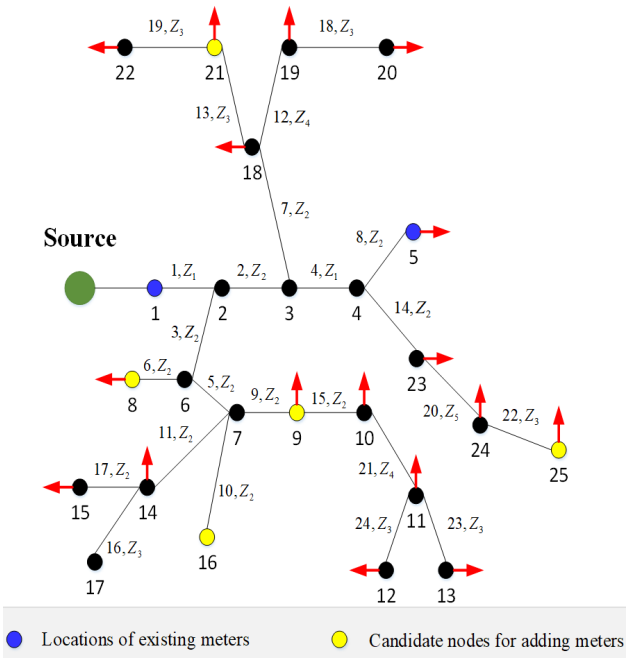

Fig. 2. The single-line diagram of the 25-node distribution test system.

considering four voltage measuring units resulting in an optimum solution vector indicating the nodes 16 and 21 as the best places for installing two additional voltage meters. Accordingly, the voltage profile under Monte Carlo scenarios corresponding to the best solution of meter places are illustrated in Figs. 3 and 4. In addition, the relative errors of the voltage magnitude and angle of the estimated states under MCS scenarios and optimal allocation of meters to nodes 1, 5, 16 and 21, are shown in Figs. 5 and 6, respectively. It is obvious from Figs. 3 and 5 that the maximum relative error between the nodal voltage magnitudes estimated by the WLS based DSSE algorithm and the actual voltage magnitude values in all MCS is less than the predefined threshold 0.01.

As seen in Fig. 6, it should be noted that the maximum relative errors of voltage angle estimates do not violate from 1% and 5% for phases b, and c, respectively, and thus $P_{\delta}^{\max}|_{b,c} = 0$. However, the relative error of the node voltage angle estimates for phase a in 18% of MCS is higher than 0.05. This indicates that the constraint (19) is violated with the probability risk index of $P_{\delta}^{\max} = 0.18$, which is less than the threshold value $p_{\delta} = 0.2$. In the preliminary analysis, the computation time of the proposed algorithm for the placement of two additional voltage meters is about 6 minutes. However, based on the minimum number of voltage meters $\left(N_{VM}^{\min} = 4\right)$, if DSO intends to have 7 meters in this feeder (which is equipped now with two measuring devices at nodes 1 and 5), the maximum number of meters must be set to 7 and the lower and upper bounds of the binary decision variables 1 and 5 are considered to be 1. To achieve this aim, the mixed-integer nonlinear problem (Eqs. (1)-(23)) can be run to find the best locations of the 5 additional meters. In the light of the above conditions, the MCS and WLS-DSSE hybrid NOMADS algorithm are converged to four optimum solution vectors, as presented in Table 5.

As discussed in Section 2 and according to Eqs. (20) and (21), the proposed algorithm is able to update the maximum and minimum number of meters required for satisfying the observability constraint Eq. (18) and fulfilling the probability of estimation error violation limit (Eq. (19)). Thus, to provide different case studies, it is supposed that DSO aims to add five meters to the radial feeder at iteration 1, as presented in Table 5. The proposed algorithm converges to a good solution vector at less than 35 minutes. The best locations for allocation of these meters are the nodes 8, 9, 16, 21 and 25. By generating 1000 Monte Carlo scenarios for nodal voltages 1, 5, 8, 9, 16, 21 and 25 (based on their reported load flow results in Table 3), the DSSE algorithm is run to estimate the voltage states under the loads with 50% variance and simulated actual measurements (Eq. (17)). It is noteworthy here that both risk indices $P_{V}^{\max}$ and $P_{\delta}^{\max}$ are zero and thus, the binary solution vector is saved as global optimal meter placement solution. It is obvious that when the DSSE algorithm converges to good estimates with lower voltage estimation errors, the distribution system will be full observable in all Monte Carlo scenarios of the best solution found in iteration 1 (iter=1) and non-singularity of the gain matrix is fulfilled in each MCS. It should be noted that each iteration of the proposed algorithm (i.e., iter) consists of an inner loop for running the NOMADS method with iterations denoted by k. To ensure the global optimality of the obtained solution at

Table 5. Optimal scenario of meter places considering $N_{VM}^{\min} = 4$ and $N_{VM}^{\max} = 7$ to allocate five additional meters in the test feeder.

iter		1	2	3	4
Max. meters number		7	6	5	4
Is the observability constraint Eq. (17) satisfied?		Yes	Yes	Yes	Yes
Meters optimal locations (node numbers)		1, 5, 8, 9, 16, 21, 25	1, 5, 9, 16, 21, 25	1, 5, 9, 16, 21	1, 5, 16, 21
Max. relative percentage error in voltage magnitudes (%)	Phase a	0.62	0.59	0.58	0.64
	Phase b	0.69	0.62	0.58	0.66
	Phase c	0.6	0.6	0.59	0.66
Max. relative percentage error in voltage phase angles (%)	Phase a	4.25	7.07	7.21	8.21
	Phase b	0.03	0.03	0.07	0.068
	Phase c	0.04	0.03	0.03	0.035
P_V^{max}		0	0	0	0
$P_\delta^{\max}$		0	6.7%	9.1%	18%
Computation time (min)		35	24	15	6

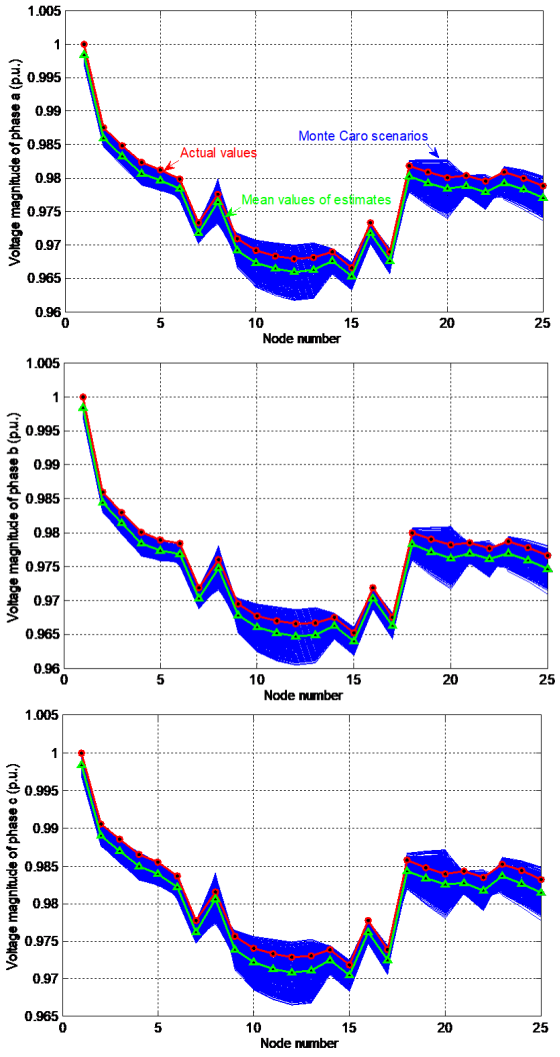

Fig. 3. Comparison between actual and estimated voltage magnitudes under MCS for optimal scenario (Nodes 1, 5, 16, 21).

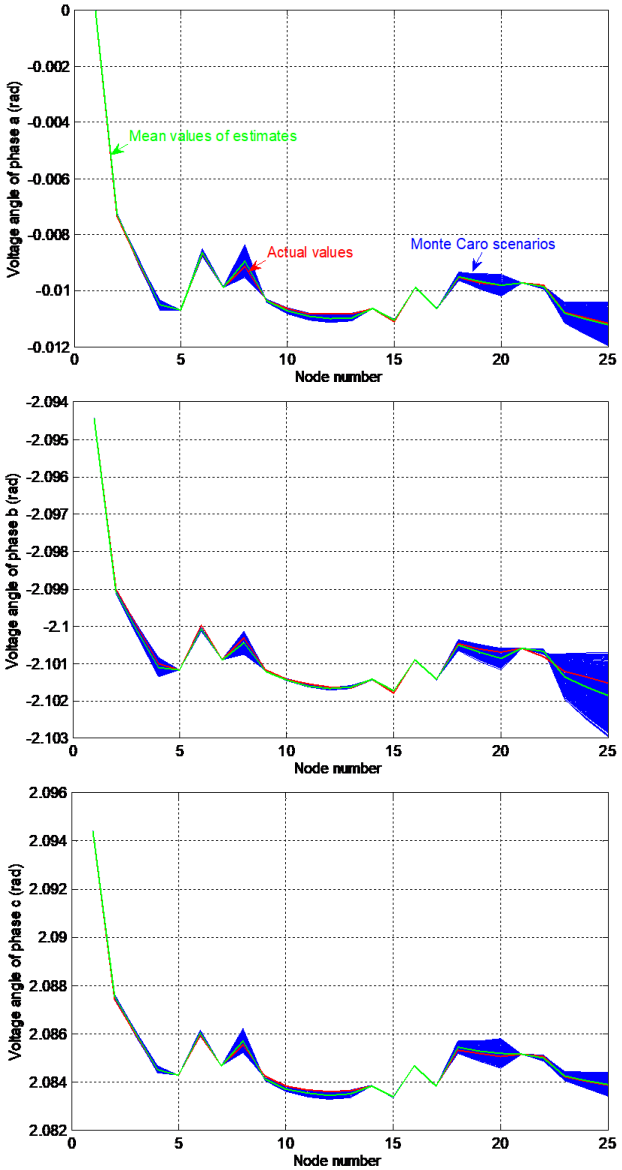

Fig. 4. Comparison between actual and estimated voltage angles under MCS for optimal scenario (Nodes 1, 5, 16, 21).

iter=1, the proposed algorithm as well as the MCS-based DSSE method are run for several times. Due to the large number of MCS, the same results presented in Table 5 are achieved with the maximum voltage magnitude and angle estimation errors of (0.62, 0.69, 0.6)% and (4.25, 0.03, 0.04)% for phases (a, b, c), respectively. These values are less than the predefined values $\varepsilon_v = 1\%$ and $\varepsilon_\delta = 5\%$ assumed for the nodal voltage magnitude and angle, respectively. According to the step (12) of Fig. 1, the number of meters is updated to 6 using Eq. (22) ($N_{VM}^{\min} = 4$ and $N_{VM}^{\max} = 7$). The 2^{nd} iteration of the meter placement algorithm (i.e., Eqs. (1)-(23)) is also run to find the best locations of the

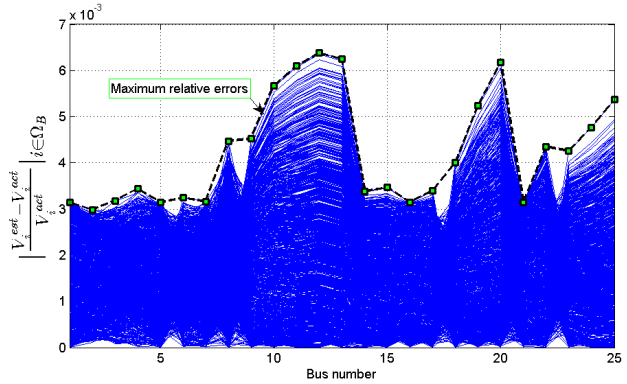

Fig. 5. Relative errors of nodal voltage magnitudes.

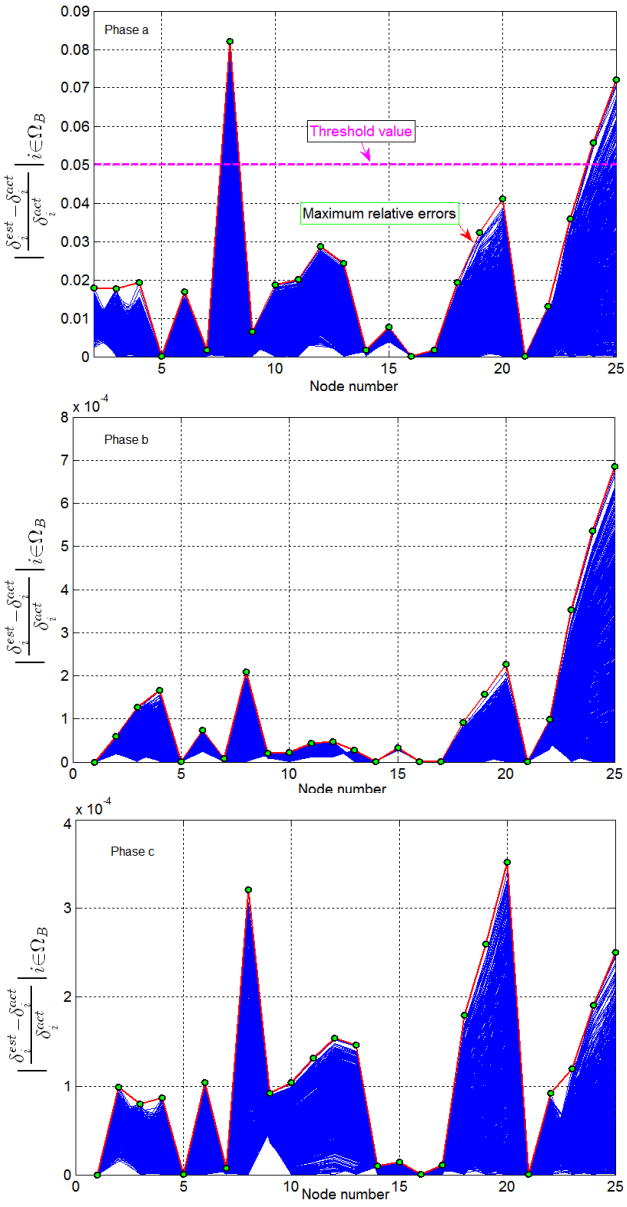

Fig. 6. Relative errors of voltage angle estimates under MCS for the optimum solution (Nodes 1, 5, 16, 21).

four additional metering devices in the radial feeder. The optimum binary decision vector demonstrates the nodes 9, 16, 21 and 25 are good candidates for measuring the voltage. The maximum voltage estimation errors are calculated for MCS and obtained respectively for each phase as (0.59, 0.62, 0.6)% and (7.07, 0.03, 0.03)%. The obtained errors are less than 1% and 5% threshold values of voltage magnitude and angle estimation relative errors, respectively. The risk indices P_V^{max} and P_V^{max} are also obtained as 0 and 6.7%, respectively. Note that in 6.7% of MCS (67 out of 1000 scenarios), the voltage angle estimation errors are higher than 5%, which is less than the probability threshold $p_V = 0.2$. Hence, the number of meters is updated similar to the iteration 2 and the algorithm is repeated with the maximum meters number of five to allocate 3 remaining measuring units in the feeder. In the 3rd iteration, the optimization model also reaches to the best locations with the acceptable risk indices. The voltage angle estimation error violates in 9.1% of MCS, which is less than 0.2. For the sake of clarity, in Table 6, the CPU time of the proposed algorithm is compared with other methods such as branch and bound (B&B) [29, 40, 41], ordinal optimization (OO) [42], multi-objective biased random-key genetic algorithm (MOBRKGA) [43], and convex relaxation of mixed-integer semi-definite programming (MISDP) [29]. The study case discussed in this paper clearly demonstrates that the proposed method in finding the optimal meter places outperforms those recently introduced methods in the literature in terms of the accuracy and computational tractability.

In case of allocating one voltage meter in test feeder with two existing meter in buses 1 and 5, the maximum relative errors of the node voltage magnitude and angle are not respectively less than 0.01 and 0.05 for more than 20% MCS of each NOMADS scenario. The minimum number of the voltage measurements is updated to be four while allocating two additional meters. Numerical results indicate that the nodes 16 and 21 as the best places for installing two additional voltage meters. The voltage profile under Monte Carlo scenarios corresponding to the best solution of meter places reveals that the relative errors of the voltage magnitude and angle of the estimated states in 80% of MCS is lower than the predefined values. In other words, two additional voltage measurement units are required to be installed for observing test distribution system with maximum relative percentage error of 1% for voltage magnitude and 5% for voltage angle in 80% of MCS. Table 6 demonstrates that the runtime of the proposed algorithm for allocating the minimum required meters in test distribution system is 6 min, which is less than those of other algorithms.

4. Concluding Remarks and Future Trends

In this paper, a novel meter placement approach was proposed based on Monte Carlo simulations, WLS-based branch currents state estimator, and an iterative nonlinear mesh adaptive direct search algorithm. For the accurate representation of the various uncertainty sources, the variability of active and reactive loads as well as the uncertainty of measured nodal voltages were considered in the optimization process. From a mathematical point of view, in this research, the minimum number of voltage meters was considered as the objective function, while the observability of the radial distribution network as well as the voltage magnitude and angle relative errors were modeled as inequality constraints. For implementation purposes, the proposed iterative NOMADS method was applied to an unbalanced radial distribution system to assess the accuracy and computational burden of the proposed method under different levels of measurement data uncertainty. From a computational viewpoint, the numerical results revealed that the proposed method technically outperforms other heuristic algorithms in the literature which are usually computationally intractable or more demanding in finding the optimal meter places under uncertainty. In addition, the iterative NOMADS enables the distribution operator to be noticed whether there are other more accurate and economic solutions than that of primitive maximum number of meters suggested. It is found that the

Table 6. The comparison between the proposed algorithm and other meter placement methods from the computational viewpoint.

Additional meter Number	2	3	4	5
Branch and Bound (B&B) [29, 40, 41]	36 min	6 h and 53 min	21 h and 51 min	> 1 day
Ordinal Optimization (OO) [42]	-	4 h and 31 min	4 h and 27 min	5 h and 49 min
Multi-Objective Biased Random-Key Genetic Algorithm (MOBRKGA) [43]	-	45 min	1 h and 50 min	3 h and 13 min
Convex relaxation of Mixed-Integer Semi-Definite Programming (MISDP) [29]	2 min	13 min	28 min	37 min
Proposed algorithm	6 min	15 min	23 min	35 min

proposed NOMADS-MCS coupled meter placement algorithm is able to allocate a limited number of meters in unobservable radial distribution systems within a relatively low runtime.

Moreover, if an optimal solution is found for a given number of meters, it then searches solutions with fewer meters until an infeasible measurement allocation scenario been found. In all scenarios, the observability of distribution feeders is also checked by the gain matrix of the DSSE algorithm in such a way that if this matrix is nonsingular, the system will be full-observable. The probability of the voltage magnitude/phase angle estimation error violation is calculated based on actual and estimated values of nodal voltages, and should be less than the predefined values. One of the main advantages of the proposed approach is the time saving and accuracy of the estimated states, which makes it possible to monitor the near real-time status of the radial distribution feeders. As future works, the researchers and practitioners should consider the lack of information in distribution feeders (e.g., GIS data) in their placement strategies, especially at low voltage levels. Moreover, there is still a need that the effects of pseudo-measurements on state estimation algorithms are alleviated by introducing some other novel approaches. Additionally, for the accurate representation of the various uncertainty sources, it is suggested to take into account uncertainties relevant to unforeseen disturbances occurring in real-time (e.g., the outage of DGs, branches, and metering device), sudden variations of the system load, or daily changes of network topology due to the connection of new customers. Last but not least, more attention needs to be paid on simultaneously allocation of different types of measurements with different time resolutions in power distribution networks. The cyber-physical security of the smart distribution feeders should be assessed using the DSSE and point estimation method based false data injection or intrusion detection techniques. In addition, large normalized residuals of actual measurements can be used as key indices to detect bad data.

ACKNOWLEDGMENTS

This work is supported by Niroo Research Institute (NRI) under Contract No. 9850108 and QC No. CPBDA01.

REFERENCES

[1] F. Jabari, B. Mohammadi Ivatloo, B. Sharifian, and H. Ghaebi, "Day-ahead economic dispatch of coupled desalinated water and power grids with participation of compressed air energy storages," *J. Oper. Autom. Power Eng.*, vol. 7, no. 1, pp. 40–48, 2019.

[2] A. Angioni, J. Shang, F. Ponci, and A. Monti, "Real-time monitoring of distribution system based on state estimation," *IEEE Trans. Instrum. Meas.*, vol. 65, no. 10, pp. 2234–2243, 2016.

[3] F. Jabari, A. Bahmanyar, and M. Shabanzadeh, "Optimal meter placement in distribution feeders using branch-current based three-phase state estimation: A quest for observability enhancement," in *10th Smart Grid Conf. (SGC)*, pp. 1–6, IEEE, 2020.

[4] K. Amiri and R. Kazemzadeh, "Enhancement of two-step state estimation performance in unbalanced distribution networks," *Comput. Electr. Eng.*, vol. 86, p. 106724, 2020.

[5] F. Jabari, M. Zeraati, M. Sheibani, and H. Arasteh, "Robust self-scheduling of pvs-wind-diesel power generation units in a standalone microgrid under uncertain electricity prices," *J. Oper. Autom. Power Eng.*, vol. 12, no. 2, pp. 152–162, 2024.

[6] G. N. Korres and N. M. Manousakis, "A state estimator including conventional and synchronized phasor measurements," *Comput. Electr. Eng.*, vol. 38, no. 2, pp. 294–305, 2012.

[7] P. Janssen, T. Sezi, and J.-C. Maun, "Meter placement impact on distribution system state estimation," 2013.

[8] M. Zeraati, M. Shabanzadeh, M. R. Sheibani, and F. Jabari, "Meter placement algorithms to enhance distribution systems state estimation: Review, challenges and future research directions," *IET Renewable Power Gener.*, vol. 16, no. 15, pp. 3422–3444, 2022.

[9] A. Al-Wakeel, J. Wu, and N. Jenkins, "State estimation of medium voltage distribution networks using smart meter measurements," *Appl. Energy*, vol. 184, pp. 207–218, 2016.

[10] R. Singh, B. C. Pal, and R. B. Vinter, "Measurement placement in distribution system state estimation," *IEEE Trans. Power Syst.*, vol. 24, no. 2, pp. 668–675, 2009.

[11] M. G. Damavandi, V. Krishnamurthy, and J. R. Martí, "Robust meter placement for state estimation in active distribution systems," *IEEE Trans. Smart Grid*, vol. 6, no. 4, pp. 1972–1982, 2015.

[12] F. C. Schweppe and J. Wildes, "Power system static-state estimation, part i: Exact model," *IEEE Trans. Power Appar. Syst.*, no. 1, pp. 120–125, 1970.

[13] P. M. Joshi and H. Verma, "Synchrophasor measurement applications and optimal pmu placement: A review," *Electr. Power Syst. Res.*, vol. 199, p. 107428, 2021.

[14] M. Nazari-Heris and B. Mohammadi-Ivatloo, "Application of heuristic algorithms to optimal pmu placement in electric power systems: An updated review," *Renewable Sustainable Energy Rev.*, vol. 50, pp. 214–228, 2015.

[15] A. Aziz, S. Khalid, M. Mustafa, H. Shareef, and G. Aliyu, "Artificial intelligent meter development based on advanced metering infrastructure technology," *Renewable Sustainable Energy Rev.*, vol. 27, pp. 191–197, 2013.

[16] F. Jabari, B. Mohammadi Ivatloo, B. Sharifian, and H. Ghaebi, "Optimal short-term coordination of desalination, hydro and thermal units," *J. Oper. Autom. Power Eng.*, vol. 7, no. 2, pp. 141–147, 2019.

[17] X. Chen, J. Lin, C. Wan, Y. Song, S. You, Y. Zong, W. Guo, and Y. Li, "Optimal meter placement for distribution network state estimation: A circuit representation based

milp approach," *IEEE Trans. Power Syst.*, vol. 31, no. 6, pp. 4357–4370, 2016.

[18] D. M. Ferreira, P. M. Carvalho, and L. A. Ferreira, "Optimal meter placement in low observability distribution networks with der," *Electr. Power Syst. Res.*, vol. 189, p. 106707, 2020.

[19] N. Khanjani and S. M. Moghaddas-Tafreshi, "An ilp model for stochastic placement of μpmus with limited voltage and current channels in a reconfigurable distribution network," *Int. J. Electr. Power Energy Syst.*, vol. 148, p. 108951, 2023.

[20] A. C. Tapia and A. R. Messina, "Constrained sensor placement and state reconstruction in power systems from partial system observations," *Int. J. Electr. Power Energy Syst.*, vol. 146, p. 108720, 2023.

[21] N. Veerakumar, D. Ćetenović, K. Kongurai, M. Popov, A. Jongepier, and V. Terzija, "Pmu-based real-time distribution system state estimation considering anomaly detection, discrimination and identification," *Int. J. Electr. Power Energy Syst.*, vol. 148, p. 108916, 2023.

[22] A. Hassannejad Marzouni, A. Zakariazadeh, and P. Siano, "Measurement devices allocation in distribution system using state estimation: A multi-objective approach," *Int. Trans. Electr. Energy Syst.*, vol. 30, no. 8, p. e12469, 2020.

[23] J. Liu, F. Ponci, A. Monti, C. Muscas, P. A. Pegoraro, and S. Sulis, "Optimal meter placement for robust measurement systems in active distribution grids," *IEEE Trans. Instrum. Meas.*, vol. 63, no. 5, pp. 1096–1105, 2014.

[24] S. Prasad and D. M. Vinod Kumar, "Robust meter placement for active distribution state estimation using a new multi-objective optimisation model," *IET Sci. Meas. Technol.*, vol. 12, no. 8, pp. 1047–1057, 2018.

[25] H. Rosli, H. Mokhlis, K. Naidu, J. Jamian, and A. H. A. Bakar, "Improving state estimation accuracy through incremental meter placement using new evolutionary strategy," *Arabian J. Sci. Eng.*, vol. 39, pp. 7981–7989, 2014.

[26] H. Wang, W. Zhang, and Y. Liu, "A robust measurement placement method for active distribution system state estimation considering network reconfiguration," *IEEE Trans. Smart Grid*, vol. 9, no. 3, pp. 2108–2117, 2016.

[27] S. Prasad and V. K. Dulla Mallesham, "Multi-objective hybrid estimation of distribution algorithm-interior point method-based meter placement for active distribution state estimation," *IET Gener. Trans. Distrib.*, vol. 12, no. 3, pp. 767–779, 2018.

[28] A. A. Raposo, A. B. Rodrigues, and M. d. G. da Silva, "Optimal meter placement algorithm for state estimation in power distribution networks," *Electr. Power Syst. Res.*, vol. 147, pp. 22–30, 2017.

[29] Y. Yao, X. Liu, and Z. Li, "Robust measurement placement for distribution system state estimation," *IEEE Trans. Sustainable Energy*, vol. 10, no. 1, pp. 364–374, 2017.

[30] M. M. Othman, M. Ahmed, and M. Salama, "A novel smart meter technique for voltage and current estimation in active distribution networks," *Int. J. Electr. Power Energy Syst.*, vol. 104, pp. 301–310, 2019.

[31] A. Ketabi, M. R. Sheibani, and S. M. Nosratabadi, "Power quality meters placement using seeker optimization algorithm for harmonic state estimation," *Int. J. Electr. Power Energy Syst.*, vol. 43, no. 1, pp. 141–149, 2012.

[32] L. Ibarra, J. Avilés, D. Guillen, J. Mayo-Maldonado, J. Valdez-Resendiz, and P. Ponce, "Optimal micro-pmu placement and virtualization for distribution network changing topologies," *Sustainable Energy Grids Networks*, vol. 27, p. 100510, 2021.

[33] V. S. Tabar, S. Tohidi, S. Ghassemzadeh, and P. Siano, "Enhancing security and observability of distribution systems with optimal placement of μpmus and firewalls," *Int. J. Electr. Power Energy Syst.*, vol. 135, p. 107601, 2022.

[34] A. Rabiee, "An advanced state estimation method using virtual meters," *J. Oper. Autom. Power Eng.*, vol. 5, no. 1, pp. 11–18, 2017.

[35] K. Mazlumi, M. Mohammad Gholiha, R. Abbasi, and F. Mazlumi, "Presenting a new method based on branch placement for optimal placement of phasor measurement units," *J. Oper. Autom. Power Eng.*, vol. 2, no. 1, pp. 32–39, 2014.

[36] O. Eghbali, R. Kazemzadeh, and K. Amiri, "Multi-area state estimation based on pmu measurements in distribution networks," *J. Oper. Autom. Power Eng.*, vol. 8, no. 1, pp. 65–74, 2020.

[37] C. Audet, V. Béchard, and S. L. Digabel, "Nonsmooth optimization through mesh adaptive direct search and variable neighborhood search," *J. Global Optim.*, vol. 41, pp. 299–318, 2008.

[38] S. A. Taher and R. Bagherpour, "A new approach for optimal capacitor placement and sizing in unbalanced distorted distribution systems using hybrid honey bee colony algorithm," *Int. J. Electr. Power Energy Syst.*, vol. 49, pp. 430–448, 2013.

[39] C. Audet, G. Couture, and J. Dennis Jr, "Nomad project (ltmads package)," *Software Available www. gerad. ca/nomad*.

[40] E. L. Lawler and D. E. Wood, "Branch-and-bound methods: A survey," *Oper. Res.*, vol. 14, no. 4, pp. 699–719, 1966.

[41] J. Lofberg, "Yalmip: A toolbox for modeling and optimization in matlab," in *2004 IEEE Int. Conf. Rob. Autom. (IEEE Cat. No. 04CH37508)*, pp. 284–289, IEEE, 2004.

[42] R. Singh, B. C. Pal, R. A. Jabr, and R. B. Vinter, "Meter placement for distribution system state estimation: An ordinal optimization approach," *IEEE Trans. Power Syst.*, vol. 26, no. 4, pp. 2328–2335, 2011.

[43] A. A. Raposo, A. B. Rodrigues, and M. d. G. da Silva, "Robust meter placement for state estimation considering distribution network reconfiguration for annual energy loss reduction," *Electr. Power Syst. Res.*, vol. 182, p. 106233, 2020.